

A NEW NON-REDUNDANT SCALE INVARIANT INTEREST POINT DETECTOR

Luis Ferraz

Department of Computing Science, Universitat Autònoma de Barcelona, Barcelona, Spain

Xavier Binefa

Department of Information and Communication Technologies, Universitat Pompeu Fabra, Barcelona, Spain

Keywords: Interest points extraction, Gaussian curvature, Scale space.

Abstract: In this paper we present a novel scale invariant interest point detector of blobs which incorporates the idea of blob movement along the scales. This trajectory of the blobs through the scale space is shown to be valuable information in order to estimate the most stable locations and scales of the interest points. Our detector evaluates interest points in terms of their self trajectory along the scales and its evolution avoiding redundant detections. Moreover, in this paper we present a differential geometry view to understand how interest points can be detected. We propose analyze the gaussian curvature to classify image regions as elliptical (blobs) or hyperbolic (corners or saddles). Our interest point detector has been compared with Harris-Laplace and Hessian-Laplace detectors on infrared (IR) images, outperforming their results in terms of the number and precision of interest points detected.

1 INTRODUCTION

Interest point detection algorithms have been shown to be well suited for feature extraction. The main goal of these algorithms is to allow the extraction of features invariant to some viewing conditions. Scale invariant detectors estimate the location and the scale of these features. Different scale invariant detectors have been developed over the past few years and among the most important we can find Laplacian of Gaussian (LoG) (Lindeberg, 1998), Derivative of Gaussian (DoG) (Lowe, 2004), Harris-Laplace (Mikolajczyk and Schmid, 2004), Hessian-Laplace (Mikolajczyk et al., 2005) or Maximally Stable Extremal Regions (MSER) (Matas et al., 2002).

MSER produces good results in comparison with other detectors but it is not analyzed in this paper because of its bad performance on blurred images (Mikolajczyk et al., 2005).

Typically, these detectors are based on a multi-scale analysis of the image (Crowley, 1982). The space-scale can be built using different scale normalized operators, like Laplace filters or difference of Gaussians filters. For these detectors an interest point is detected if a local 3D extreme is present and if its

absolute value is higher than a threshold. Therefore, blobs at different scales are not related and the same blob can be detected many times along the scale-space. To avoid this problem, our proposal is to estimate the trajectory of blobs along scales and select the scale and location that best represent each blob.

From a differential geometry point of view images can be understood as surfaces with 3 types of regions in function of their gaussian curvature: elliptical regions, parabolic regions and hyperbolic regions. These types of regions allow to see images in a simple way, where elliptical regions can be understood as blobs, parabolic regions as contours or plane regions and hyperbolic regions as corners or saddles.

In order to extract this differential structure we use the full Hessian matrix (DoCarmo, 1976) for each point. This approach outperforms Laplacian based operators more related to obtain rotational invariant information (Lenz, 1992).

This paper is organized as follows. In section 2 the method to detect interest points by means of curvature analysis is introduced. In section 3 our scale invariant interest point detector is described and finally, in Section 4 we present experimental results.

2 CURVATURE ANALYSIS

The image behavior in a local neighborhood of a point x_0 can be obtained by the second order Taylor approach,

$$f(\vec{x}) = f(\vec{x}_0) + \nabla f(\vec{x}_0)(\vec{x} - \vec{x}_0) + \frac{1}{2} \nabla^2 f(\vec{x}_0)(\vec{x} - \vec{x}_0)^2 + R(\vec{x}) \quad (1)$$

where the second term contains information about the gradient distribution in a local neighborhood. Using this gradient information can be computed the first fundamental form I (Equation 2). The next term is the second fundamental form II (Equation 3) that contains information about the shape near to x_0 . The last term $R(x)$ is referred to as the remainder, since it contains the difference between the image $f(\vec{x})$ and its representation.

$$I(\vec{x}_0, \sigma) = \begin{pmatrix} 1 + f_x^2(\vec{x}_0, \sigma) & f_x f_y(\vec{x}_0, \sigma) \\ f_y f_x(\vec{x}_0, \sigma) & 1 + f_y^2(\vec{x}_0, \sigma) \end{pmatrix} \quad (2)$$

$$II(\vec{x}_0, \sigma) = \begin{pmatrix} f_{xx}(\vec{x}_0, \sigma) & f_{xy}(\vec{x}_0, \sigma) \\ f_{yx}(\vec{x}_0, \sigma) & f_{yy}(\vec{x}_0, \sigma) \end{pmatrix} \quad (3)$$

where σ is the scale normalization factor for the space-scale.

The first and second fundamental forms of a surface determine an important differential-geometric invariant, the Gaussian curvature K . The Gaussian curvature of a point on a surface is the product of the principal curvatures, $K = k_1 * k_2$ of the given point. Moreover, Gaussian curvature can be expressed as the ratio of the determinants of the second and first fundamental forms,

$$K = \frac{\det(II)}{\det(I)} \quad (4)$$

The sign of the Gaussian curvature at a point determines the shape of the surface near that point (Do-Carmo, 1976): for $K > 0$ the surface is locally convex (blob regions) and the point is called elliptic, while for $K < 0$ the surface is saddle shaped (i.e. corners) and the point is called hyperbolic. The points at which the Gaussian curvature is zero (i.e. contours) are called parabolic.

The first fundamental form is positive definite, hence its determinant is positive everywhere. Therefore, the sign of K coincides with the sign of the determinant of the second fundamental form. Assuming that point \vec{x}_0 is a critical point (the gradient $\nabla f(\vec{x}_0)$ vanishes) the Gaussian curvature of the surface at \vec{x}_0 is the determinant of $II(\vec{x}_0)$. So, it is not necessary to calculate $I(x_0)$ to estimate the Gaussian curvature.

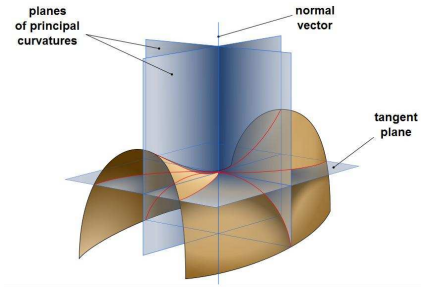


Figure 1: Saddle surface with normal planes in directions of principal curvatures.

In Figure 1 is shown the meaning of curvature. Given the normal vector to the point \vec{x}_0 , its tangent plane and its two principal curvatures k_1 and k_2 Gaussian curvature is defined positive if both curvatures have the same sign, negative if they have different sign and zero if any curvature is zero.

3 OUR INTEREST POINT DETECTOR OF BLOBS

In this section we propose a new scale invariant interest point detector of blobs based on the analysis of Gaussian curvature of the image along the space-scale representation. Moreover, to obtain more stable interest points the trajectory of each one is extracted.

The evolution of blobs along scales was studied in depth by (Lindeberg, 1993). Traditionally, the analysis of the behavior of blobs presents severe complications, since it implied a detailed description of the image. However, for our purposes we do not need a precise description and one of the important contributions of our work is to reduce the detail of the analysis since we only need an approximation of the movement of blobs.

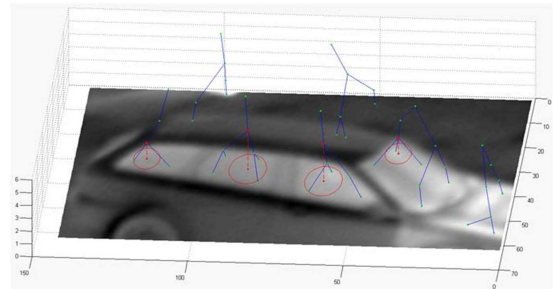


Figure 2: Trajectory of some blobs along scales (blue lines). Blob movements and blob fusions can be seen. Green points show all the extremes found. Red points are the extremes selected as interest points.

To obtain this approximation, in first place a

space-scale representation must be build. Scale normalized second fundamental form (Equation 3) is used in order to obtain it calculating the Gaussian curvature K associated to each point of each scale.

All the maxima are computed for each scale to find all the blobs. Once obtained, they must be analyzed to put them in correspondence. Blobs found in consecutive scales are linked using a gradient ascent propagation algorithm to find the nearest and plausible link. As a result of this step, the pipe/trajectory of each blob is obtained. Experimentally, we have seen that using this simple strategy provides a coherent and good approximation of the trajectories.

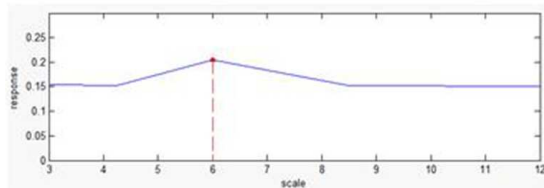


Figure 3: Example of values for the Gaussian curvature along scales given one blob trajectory.

The last step consists on obtaining from each blob trajectory which are those locations that maximize their Gaussian curvature compared with their nearest neighbors in the pipe (Figure 3).

4 EXPERIMENTAL RESULTS

IR images are thermal images that contain a high signal to noise ratio and a lack of contrast, so blurred images are obtained. We have compared our method with two typical interest point detectors that have proved, accordingly to literature, that produce good results: Harris-Laplace and Hessian-Laplace. The first one is based on the detection of corners that are representative along the space-scale and the second one on the detection of blobs.

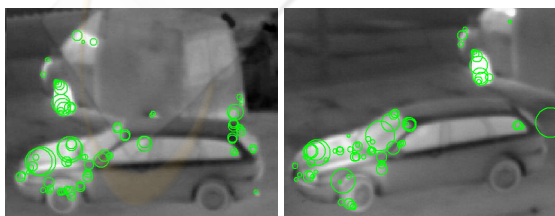


Figure 4: Example of interest points detected using Harris-Laplace detector (green circles symbolize location and scale) on two different images of an IR sequence. Comparing detected points on the images is shown that interest points are unstable.

Harris-Laplace detector calculates corners at the different scales using a scale adapted Harris operator. After that, locations of detected corners are evaluated with a Laplacian filter in the superior and inferior scales. Interest points correspond to corners with a maximal response of Laplacian filter.

Harris-Laplace detector has been applied on IR images to test its performance on these images. As Harris-Laplace detector is based on Harris operator and therefore, since in IR images corners are not sharpened, it produces bad results in contrast with Hessian-Laplace. Figure 4 show that Harris-Laplace detector produces unstable interest points in IR images. Therefore, the same object viewed from different locations and scales. Moreover, Figure 4 shows that the same interest point is detected in different scales using this detector.

Hessian-Laplace detector works in a similar way to Harris-Laplace detector (Mikolajczyk et al., 2005). The main difference is that instead of Harris operator uses a function based on the determinant of the Hessian matrix to penalize very long structures (for example it is useful to discard contours detected as blobs).

Given that Harris-Laplace produces unstable results the final comparison has been done between Hessian-Laplace detector and our blob detector. These two detectors are based on the detection of blobs, differing in two ways: the method to decide which neighbors around extremes must be analyzed and the function applied to extreme detection.

Comparing Hessian-Laplace and our detector is where the power of our algorithm is shown in a best way. Figure 5 compare these two algorithms showing that Hessian-Laplace detects a high quantity of interest points being the most of them redundant. Our detector practically does not produce redundancy because of trajectory of blobs gives information about the best scale. Moreover, our detector seems to find interest points closest to our perception that the other one.

5 CONCLUSIONS

We have presented a powerful mechanism to detect the most stable locations of blobs by estimating their trajectory along scales. By means of this trajectory the best locations and scales for each point can easily be selected. Moreover, by using the Gaussian curvature we classify regions on images in a simple way.

We have shown that over IR images those interest point detectors based on corner detection do not

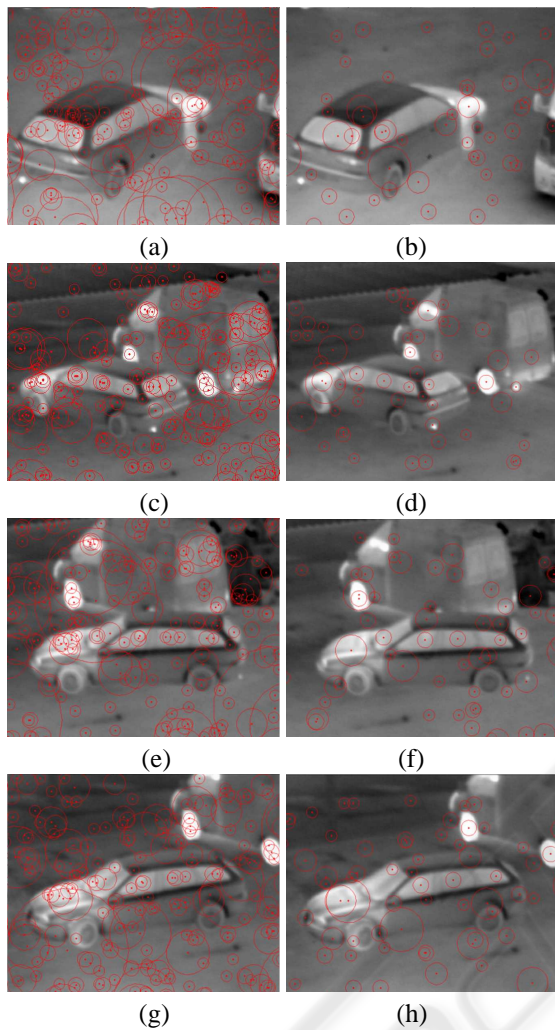


Figure 5: Hessian-Laplace versus our detector. (a), (c), (e) and (g) show the Hessian-Laplace results over 4 IR images. (b), (d), (f) and (h) show the results of our detector over the same 4 IR images. Red circles symbolize the locations and scales of interest points.

produce satisfactory results, due to the lack of sharpness of the contours. It is also a fact that interest point detectors based on blob detection, although they produce good results, most of them are redundant.

By comparing these blob detectors with our proposed detector we show that our algorithm works fine, producing promising results. It also opens future research lines around blob trajectories along scales and Gaussian curvature analysis using first and second fundamental forms. Moreover, an extension to the detection of affine blobs could be done by analyzing in depth the Gaussian curvature surface generated around each interest point.

Finally, we want to remark that our detector has been tested mainly on IR images. However, tests done

on gray level images have produced similar results.

ACKNOWLEDGEMENTS

This work was produced thanks to the support of the Universitat Autònoma de Barcelona. Thanks are also due to TecnoBit S.L. for yielding the car sequence images.

REFERENCES

- Crowley, J. L. (1982). *A representation for visual information with application to machine vision*. PhD thesis.
- DoCarmo, M. P. (1976). *Differential Geometry of Curves and Surfaces*. Prentice-Hall.
- Lenz, R. (1992). Group theoretical feature extraction: Weighted invariance and texture analysis. In *Theory & Applications of Image Analysis: Selected Papers from the 7th Scandinavian Conference on Image Analysis*, pages 63–70.
- Lindeberg, T. (1993). *Scale-Space Theory in Computer Vision (The International Series in Engineering and Computer Science)*. Springer.
- Lindeberg, T. (1998). Feature detection with automatic scale selection. *International Journal of Computer Vision*, 30:77–116.
- Lowe, D. G. (2004). Distinctive image features from scale-invariant keypoints. *International Journal of Computer Vision*, 60:91–110.
- Matas, J., Chum, O., Urban, M., and Pajdla, T. (2002). Robust wide baseline stereo from maximally stable extremal regions. In *In British Machine Vision Conference*, pages 384–393.
- Mikolajczyk, K. and Schmid, C. (2004). Scale & affine invariant interest point detectors. *International Journal of Computer Vision*, 60:63–86.
- Mikolajczyk, K., Tuytelaars, T., Schmid, C., Zisserman, A., Matas, J., Schaffalitzky, F., Kadir, T., and Van Gool, L. (2005). A comparison of affine region detectors. *International Journal of Computer Vision*, 65:43–72.